JOURNAL OF KUFA–PHYSICS
journal.uokufa.edu.iq/index.php/jkp/index | ISSN: 2077–5830

Study the Optical and Morphological Properties of (PMMA/PS/Al_2O_3) Nanocomposites Before and After Exposed to Argon Plasma

Fatima Mohammad Nayef **Bahaa H. Rabee**

Department of Physics, College of Education for Pure Sciences, University of Babylon, Iraq

*Corresponding Author E-mail: fatima466m@gmail.com

ARTICLE INF.

Article history:
Received: 13 JUL., 2023
Revised: 26 AUG., 2023
Accepted: 09 SEP., 2023
Available Online: 18 DEC.,2023

Keywords:

PMMA
Polystyrene PS
Al_2O_3
Nanocomposite
Optical characteristic

ABSTRACT

This study aimed to investigate the alterations in the structural and optical properties of Poly-methyl-methacrylate (PMMA) and Polystyrene (PS) through the utilization of different weight percentages of Aluminum oxide (Al_2O_3) nanoparticles (2%, 4%, 6%, and 8%) by weight. The optical microscope images indicate that the distribution of nanoparticles in the blend was uniform, resulting in a continuous network within the polymer matrix. The field emission scanning electron microscope revealed that there was a connection between the interface that connects the polymer matrix and the additive. The optical properties before and after the exposure to Ar plasma exhibited that the absorbance, absorption coefficient, refractive index, extinction coefficient, dielectric constant (real, imaginary) and optical conductivity of (PMMA/PS/Al_2O_3) nanocomposites increased with the increasing of the concentrations of the Al_2O_3. The transmittance and the energy gap for indirect transition (allowed, forbidden) decreased with the increasing concentrations of Al_2O_3 nanoparticles. The optical properties after irradiation are seen to have high values compared with those before the irradiation which is attributed to the increased charge carriers and the occurrence of some bonds breaking. Finally, the results indicated that the (PMMA/PS/ Al_2O_3) nanostructures can be considered as promising materials for optoelectronics nanodevices.

DOI: https://doi.org/10.31257/2018/JKP/2023/v15.i02.12527

دراسة الخصائص البصرية والمورفولوجية للمتراكب النانوي $PMMA/PS/Al_2O_3$ قبل وبعد التعرض الى بلازما الأركون

فاطمة محمد نايف **بهاء حسين ربيع**
قسم الفيزياء ,كلية التربية للعلوم الصرفة , جامعة بابل

الـــخُـــلاصـــة

هدف هذه الدراسة إلى فحص في التغيرات في الخصائص المورفولوجية والبصرية لبولي ميثيل ميثاكريلات ($PMMA$) والبوليستايرين (PS) من خلال استخدام نسب وزنية مختلفة من جسيمات النانوية أوكسيد الألومنيوم (Al_2O_3) (2، 4، 6 و 8٪). تم تصنيع العينات باستخدام طريقة الصب بالمذيب. تشير صور المجهر الضوئي إلى أن توزيع الجسيمات النانوية في المزيج كان منتظمًا، مما أدى إلى شبكة مستمرة داخل مصفوفة . باستخدام مجهر إلكتروني لمسح انبعاث المجالي، وكشف عن وجود صلة بين مصفوفة البوليمر والمادة النانوية المضافة. أظهرت نتائج الخصائص البصرية للمتراكب النانوي قبل وبعد التعرض للإشعاع بأن الامتصاصية، معامل الامتصاص، معامل الانكسار, معامل الخمود, ثابت العزل الحقيقي والخيالي ,التوصيلية البصرية تزداد مع زيادة تركيز جسيمات النانوية Al_2O_3 . النفاذية وفجوة الطاقة للانتقال غير مباشر المسموح والممنوع تقل مع زيادة تركيز جسيمات النانوية . Al_2O_3اظهرت نتائج الخصائص البصرية بعد التعرض للبلازما لها قيم عالية وهذا يعود الى زيادة حاملات الشحنة والتي تؤدي الى تكسر بعض الاواصر. هذا يعطي انطباع جيد بانه من الممكن استخدام هذه العينات ككاشف ضوئي.

الكلمات المفتاحية:

(PMMA), بولي مثيل مثيكريلايت
(PS) بوليستايرين
(Al_2O_3) أوكسيد الالمنيوم
المتراكب النانوي
الخصائص البصرية.

1. Introduction

Mixing polymers is a key step in creating novel polymeric materials that can be applied in various situations. One of the primary advantages of utilizing a polymer blend is the ability to customize the characteristics of the end product to fulfill the demands of specific applications, a Feature that cannot be accomplished when utilizing a solitary polymer type [1, 2]. Creating a nanocomposite involves combining discrete nanoscale constituents to regulate and improve the structure and properties of the material [3]. Nanocomposites are composite materials incorporating one or more nanoparticles within their matrix. Polymer nanocomposite (PNCs) are defined as a type of material with unique properties. A polymer nanocomposite (PNCs) is a polymer or copolymer containing nanoparticles or nanofillers distributed throughout the polymer matrix. Inorganic particles are disseminated in an organic polymer matrix in at least one dimension to improve the quality attributes of the material. PNCs are a modern kind of polymer that can be used instead of traditional filled polymers. Nanocomposites' filler dispersion increases their properties significantly when compared to pure polymers, are among these properties Increased tensile strength, conductivity, and thermal stability, in addition to reduced flammability [4]. In this regards, PMMA is a widely recognized and innovative polymer. (Poly methyl methacrylate) or PMMA has gained significant popularity in glazing applications, despite its original purpose as a substitute for glass in various applications [6]. The material exhibits rigidity, possesses a transparent appearance with a lustrous surface, is among the most durable polymers, and is resistant to atmospheric conditions [7].The Polymethyl methacrylate (PMMA) exhibits high transparency and a neutral appearance. The level of transmittance of visible light is considerably high. The significance of PMMA polymeric composites in technical applications is extensively recognized [8].

Polystyrene (PS), a pliable plastic material, is extensively utilized in various industries and everyday activities due to its cost-effectiveness, lightweight nature, ease of production, flexibility, thermal efficiency, durability, and moisture resistance [9,10]. Among all known metal oxide nanomaterials, Al_2O_3 NPs have drawn remarkable attention in the cutting edge of particular innovation, in the formulation and designing of recent antimicrobial agents for sustainable biomedical applications; because Al_2O_3 NPs are chemically bio-inert and hydrolytically more stable. The biocompatibility of Al_2O_3 ceramic has already been mentioned by many researchers. Al_2O_3 NPs with high purity were the first bio-ceramics widely utilized in clinical application, and it was recommended that the lifespan of Al_2O_3 is longer than the concerned patients[4,11]. The compound of aluminum oxide (Al_2O_3) has attarcted attention for its exceptional stability, ability to withstand harsh conditions, and impressive transparency that extends to 250 nm, as reported in literature [11]. The photo-physical characteristics of these dyes in diverse solid environments, including polymers, owned significant interest owing to their potential applications as adjustable solid-state dyes, sensor and probe devices based on their physical properties, as well as their antibacterial and biological uses due to their biological attributes [12]. The interaction between organic material and polymers with electromagnetic radiation occurs through the involvement of atoms and molecules. [13]. This paper aims to presentation of the low-cost and easy synthesis process by PMMA/PS/Al_2O_3 nanostructures for optoelectronics applications.

2. Materials and Method

Using the casting approach, nanocomposites containing varying proportions of Al2O3 were fabricated. One gram of (70% poly methyl methacrylate/30%polystyrene) was dissolved in thirty milliliters of chloroform for 50 minutes, while stirring with a magnetic stirrer at a temperature of 50 °C to achieve a more homogeneous solution to create the composite film. Al_2O_3 NPs were added to a solution of PMMA and PS with weight percentages of 2%,4%,6%, and 8% to create the NCS. Upon drying the solution for a duration of three days at ambient temperature, the resultant outcome was the formation of polymer nanocomposites. The (PMMA/PS/Al2O3) nanocomposites were extracted from the petri dish and utilized for measurement. The samples were tested at varying concentrations, and an Olympus-type Nikon-73346 optical microscope with a camera for microscopic photography was utilized. Spectrophotometer (UV-18000A-Shimadzu) was used to determine the optical properties of poly methyl methacrylate/polystyrene/ Al_2O_3 NPS.

We can calculate the absorption coefficient (α) by [14]:-

$$\alpha = 2.303(A/d) \qquad (1)$$

In which: A is absorbance, and d is thickness. The energy gap was calculated by using the relation [15]:-

$$\alpha h\upsilon = B(h\upsilon - Eg)r \quad (2)$$

Where: B is constant, hυ is the incident photon energy, E_g is the optical band gap, and the value of r is 2 for allowed indirect transitions and 3 for forbidden indirect transitions.

The extinction coefficient (k) was calculated using the following equation [17]

$$k=\frac{\alpha\lambda}{4\pi} \quad (3)$$

Where: λ is the wavelength

The refractive index (n) was calculated using the following equation [18]

$$n = \sqrt{4R - \frac{k2}{(R-1)2}} - \frac{(R+1)}{(R-1)} \quad (4)$$

Where: R is the reflectance

The dielectric constant (real and imaginary parts) was calculated by [17]

$$\varepsilon 1 = n2 - k2 \quad (5)$$

$$\varepsilon 2 = 2nk \quad (6)$$

The optical conductivity (σ_{op}) was obtained by using the following relation [19]

$$\sigma op = \alpha nc/4\pi \quad (7)$$

Where: c is the velocity of light

3. Result and discussion

FTIR spectra of (PMMA/PS/Al2O3) nanocomposites are shown in figure (1) at wavenumber range (500-4000) cm-1. FTIR studies of nanocomposites show the interactions in nanocomposites. FTIR spectra of (PMMA/PS) polymer are reveals absorption band at 2984.45 cm-1 corresponding to the CH3 bending vibration and the band 1723.34 cm-1 owing to the C=O stretching vibration. Band at 1435.14 cm^{-1} corresponding to the CH3 stretching vibration. The absorption band at 1143.71 cm-1 attribute to the symmetric stretching vibration of C-O. The bands 984.77 cm-1, 697.33 cm-1 and 749.08 cm-1 matching to the C−C bending and stretching vibration respectively [20]. After adding Al2O3 nanoparticles to the polymers (PMMA/PS) as shown in image (from B to E) from fig. (1) leads to the displacement of some of the bonds and not emergence of new peaks therefore, there is no interaction between Al_2O_3 nanoparticle and the PMMA/PS polymer matrix. These results agree with the researchers [21,22].

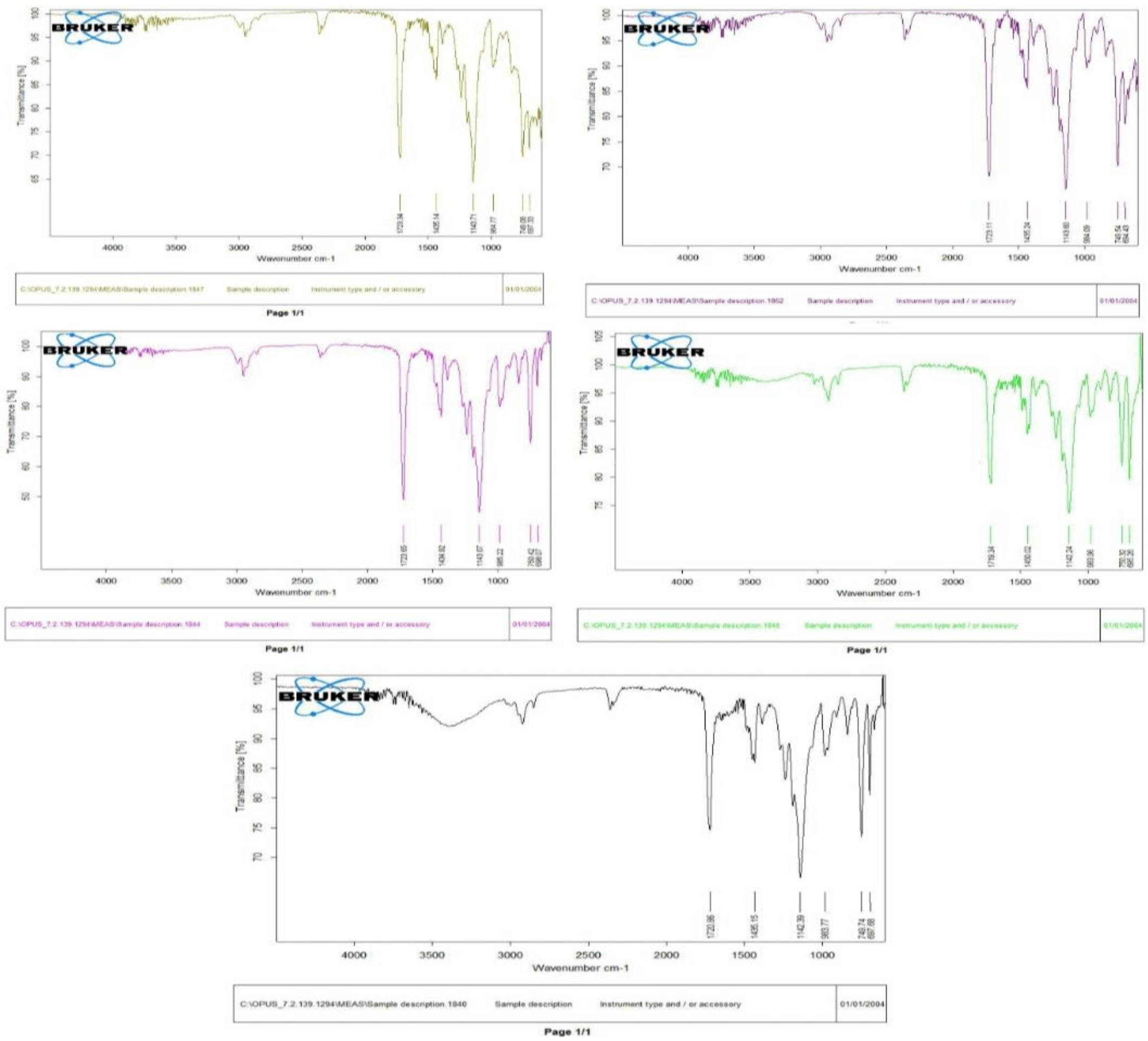

Figure (1): FTIR spectra of (PMMA/PS/) nanocomposites A. pure polymer, B. 2 wt.% of (Al_2O_3) NPs, C. 4 wt.% of (Ag) NPs, D. 6 wt.% of (Ag) NPs and E. 8 wt.% of (Al_2O_3) NPs.

The optical microscope of (Poly-methyl-methacrylate-Polystyrene)/(Al_2O_3)NPS.

The optical microscope images of Poly-methyl-methacrylate-(PMMA)/ Polystyrene(PS)/ (Al_2O_3) before and after exposure to Argon plasma are presented in Figure 2. As seen in the image, a 10X magnification was applied. Al_2O_3 nanoparticles create a continuous network when added to (Poly-methyl-methacrylate-(PMMA)/ Polystyrene (PS)) composites at a rate of 8%.

Figure(3) show that Al_2O_3NPs aggregates form at low ratios in images B, C, D, and E.

A continuous network forms in the (PMMA/PS) composites at a 8% concentration as the Al_2O_3 nanoparticles (NPs) concentration increases. Conversely, when Al_2O_3 NPS concentrations were smaller, the surface of the nanocomposite shows signs of pitting due to the exposure to Argon plasma gas. The contact of the sample's surface and the Argon plasma gas increases after it reaches a threshold of 8 weight percent of Al_2O_3NPs,

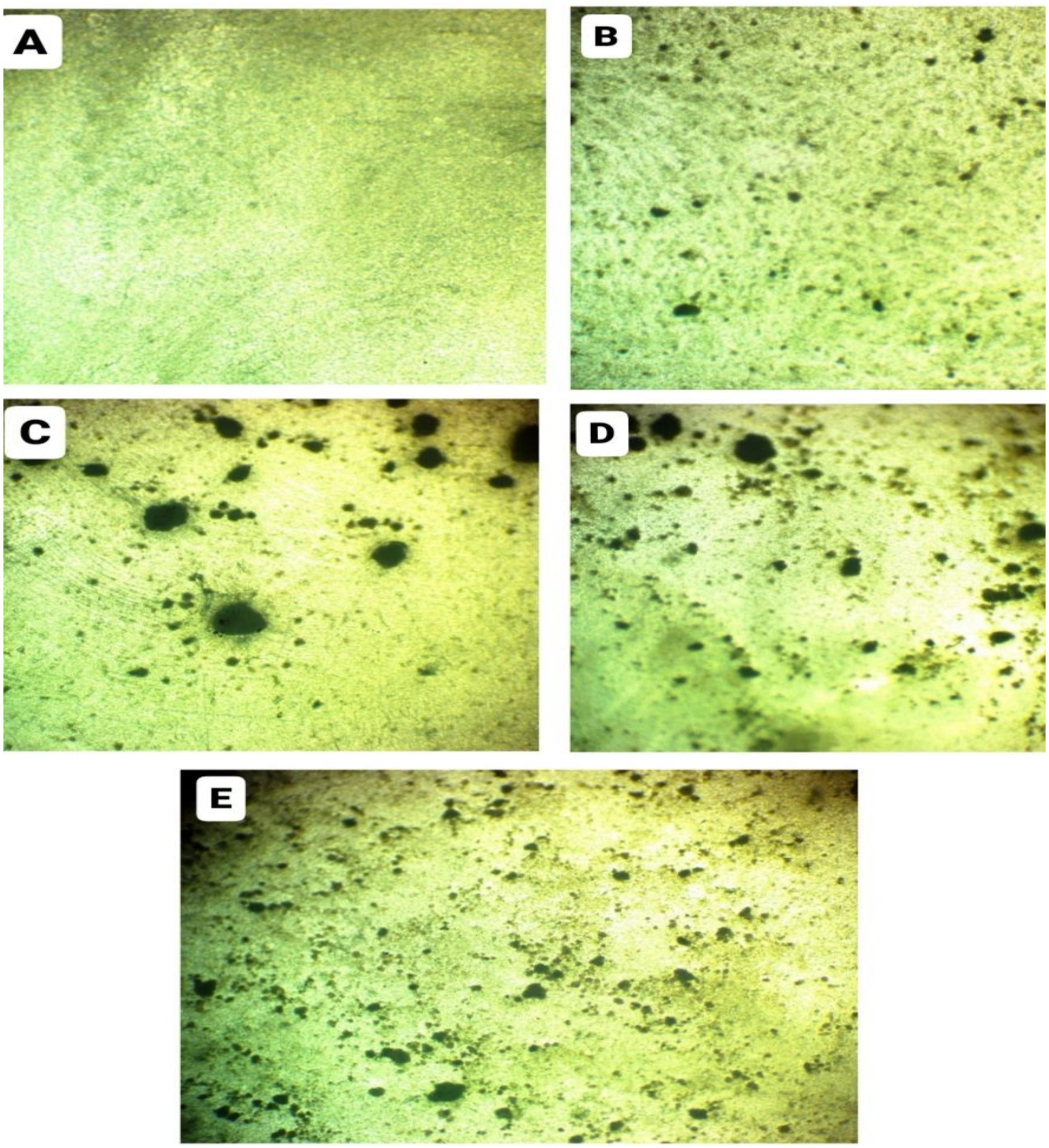

Figure(2): The optical microscope pictures at a magnification of (10X) for (Poly-methyl-methacrylate/ Polystyrene/Al_2O_3) NCS :(A:- pure) (B:- 2 wt.%), (C:- 4 wt.%), (D:- 6 wt.%) and (E:- 8 wt.%)

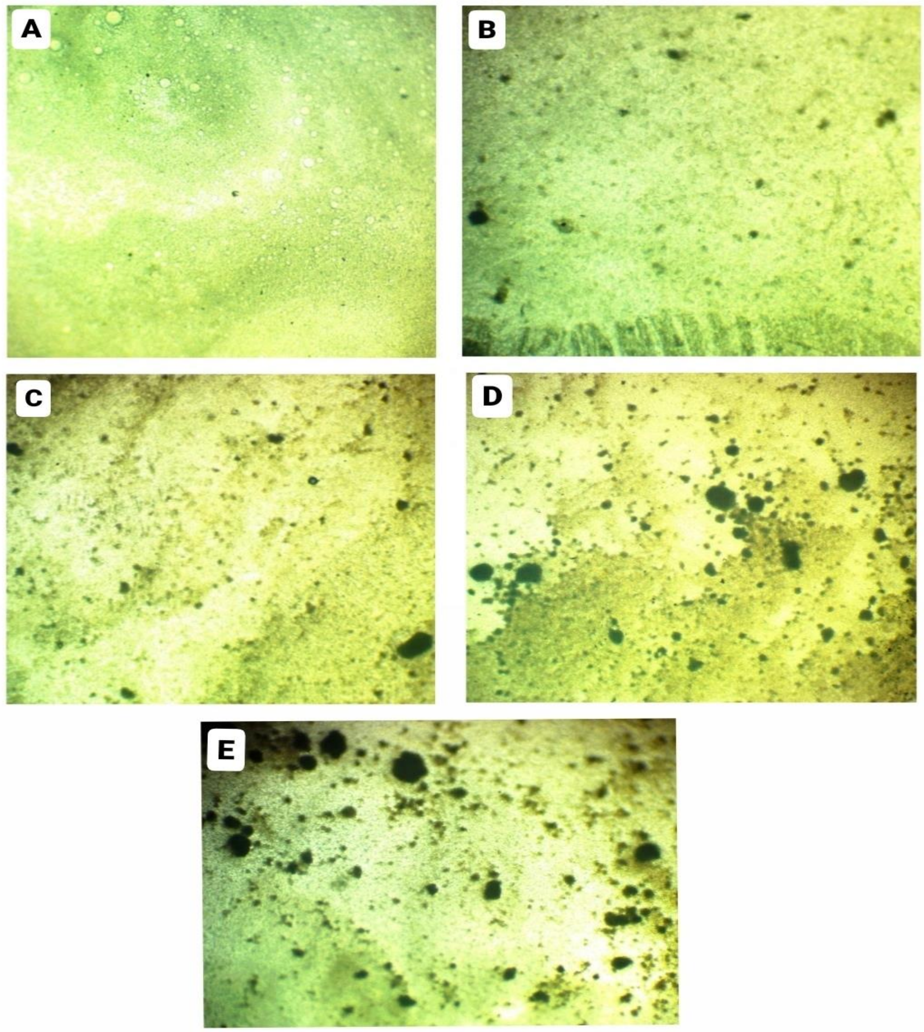

Figure (3): The optical microscope pictures at a magnification of (10X) (x10) for (Poly-methyl-methacrylate/ Polystyrene/Al_2O_3) NCS afterward bare Argon plasma: (A:- pure), (B:- 2 wt.%), (C:- 4 wt.%), (D:- 6 wt.%)and (E:- 8 wt.%)

The compatibility between different polymer and nanomaterial components was investigated using (FESEM). The investigation of the surface structure of nanocomposite samples that composed of PMMA/PS/Al_2O_3 was conducted through the utilization of (FESEM) both prior to and after to exposure to Ar plasma. The findings are depicted in Figures (4) and (5).

The obtained Results from the incorporation of Al2O3 NPS into Polymethyl methacrylate/polystyrene polymer in images (B,C,D,E) demonstrate a tendency for the nanoparticles to aggregate and generate suitably dispersed (Poly-methyl-methacrylate/Polystyrene/Aluminum oxide) NCS films. Visual representations exhibit a degree of consistency and uniformity in the resultant films, characterized by a uniform and homogeneous superficial appearance. Introducing nanoparticles into the polymer matrix led to the nanocomposites displaying advantageous dispersion properties, effectively hindering agglomeration. A significant proportion of the nanoparticles demonstrated a consistent pattern on the surface of the nanocomposite films, indicating the uniform distribution of surface morphology variations.

As depicted in Figure 5, it is evident that the emergence of holes is a consequence of the argon plasma gas's surface exposure. Furthermore, it was observed that upon attaining 8 wt.% concentration of Al_2O_3 NPs, the development of grooves occurs [20]. The utilization of reactive gases such as argon in treatments is recognized to generate this phenomenon. The procedures above entail the chemical interplay between dynamic plasma particles and the targeted sample constituents, leading to their elimination and the formation of unstable byproducts such as water vapor, carbon monoxide, and carbon dioxide. In addition, the presence of polar groups in the system could lead to their persistence in the discharge and subsequent reincorporation into the sample. This finding is consistent with the results reported in the literature [26,27].

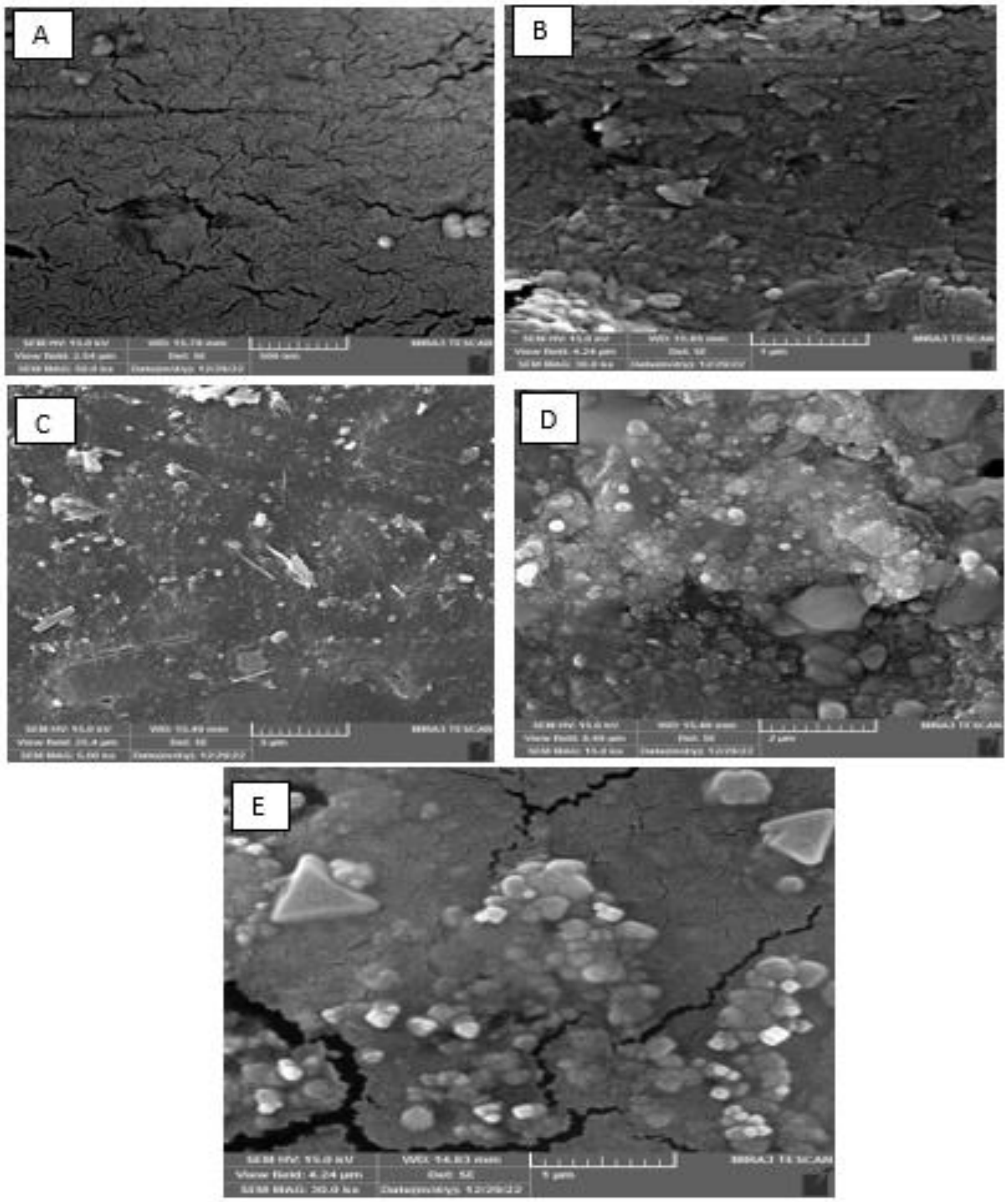

Figure (4): FESEM images of (Polymethyl methacrylate/polystyrene/Al_2O_3) NCS : (A) pure (B) 2 wt.%, (C) 4 wt.%, (D) 6 wt.% and (E) 8 wt.%.

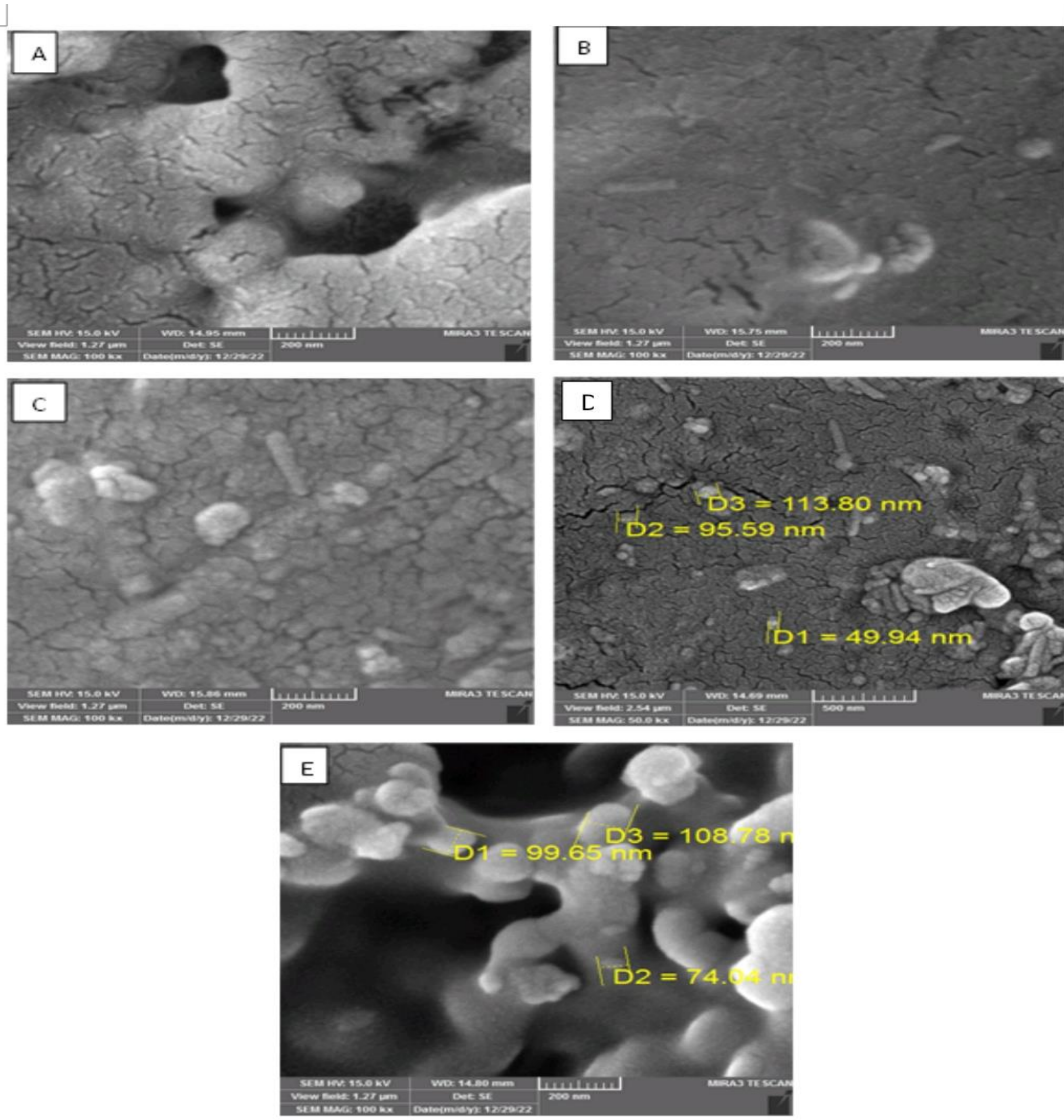

Figure (5): FESEM images of (Poly-methyl-methacrylate/Polystyrene/ Al_2O_3) NCS after exposed Ar plasma : (A:- pure), (B:- 2 wt.%), (C:- 4 wt.%), (D:- 6 wt.%) and (E:- 8 wt.%).

The Absorbance

Figures (6, 7) depict a comparison of the absorbance values over a range of 200. A comparative analysis of Poly-methyl-methacrylate/Polystyrene NCS at 1100 nm is required pre- and post-Ar plasma exposure. The Al203 relationship exhibits increased absorbency due to a higher number of charge carriers resulting from the absorption of

Poly-methyl-methacrylate/ Polystyrene/Al203 NCS materials, as unbound electrons can absorb incident light. The visible components exhibit a propensity for undergoing and experiencing bond degradation. The results agree with the research conducted by scholars 25, 26, and 27.

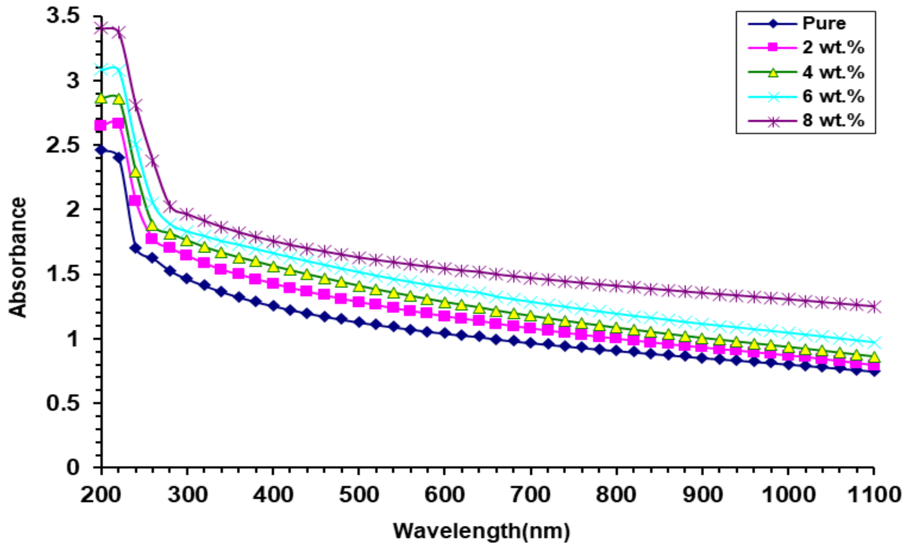

Figure (6): Absorbance of Poly-methyl-methacrylate/Polystyrene/ Al_2O_3 NCS with wavelength.

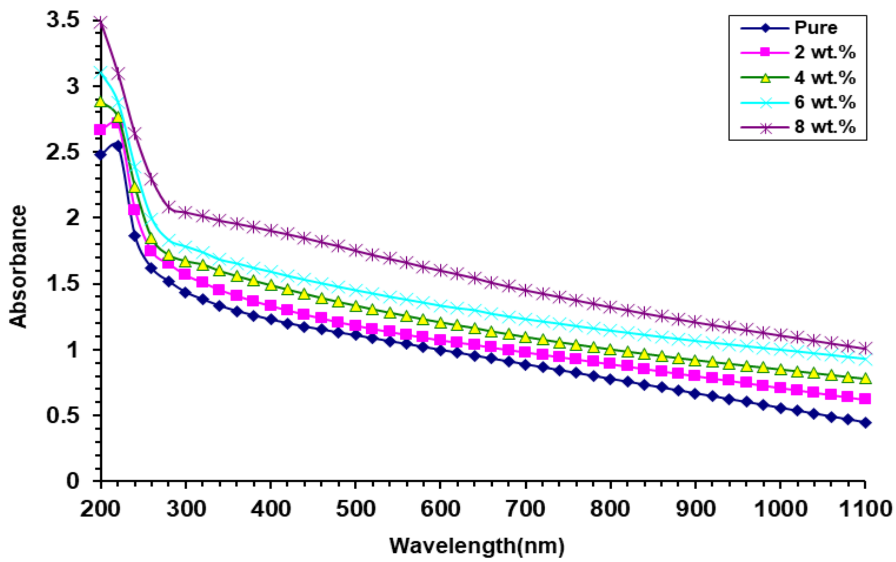

Figure (7): Absorbance of Poly-methyl-methacrylate/Polystyrene/ Al_2O_3 NCS with wavelength.

The light permeability of PMMA/PS/Al2O3 composites was depicted in Figures (8) and (9), respectively, prior to and after Ar plasma exposure. The statistical data indicates that an increase in Al2O3 concentration resulted in a corresponding increase in reflectance and a decrease in penetration. The transmission was enhanced following irradiation due to the breakdown of bonds and the presence of charge carriers. The finding is consistent with the studies conducted by researchers [26,27].

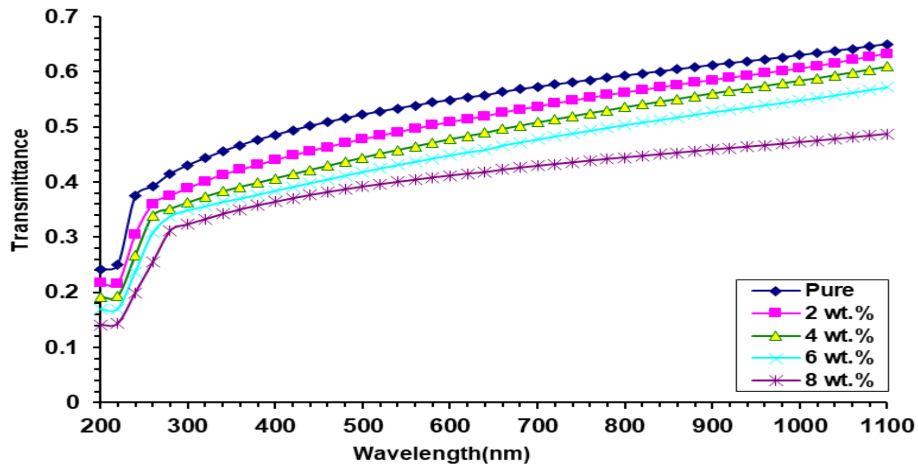

Figure (8): The transmittance of (PMMA/PS/Al_2O_3) NCS.

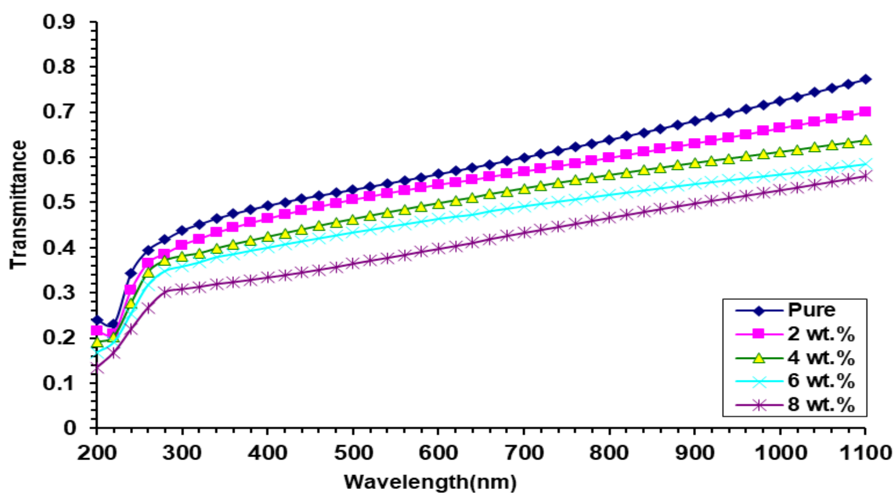

Figure (9): The transmissivity of (PMMA/PS/Al_2O_3) NCS afterward bare Ar juice.

Figures 10 and 11 depict nanotechnology's photon energy absorption coefficients comprising Poly-methyl-methacrylate, Polystyrene, and Aluminum oxide before and after undergoing Ar ionized treatment. The absorption index has the potential to indicate an electron transition. Absorbance coefficients of 104 cm^{-1} suggest rapid electron transitions. Indirect electron transition occurs under conditions of low ingestion ratio. The copolymer consisting of PMMA, PS, and Al203 exhibits an absorbance coefficient lower than 104 cm^{-1}, resulting in an indirect electron transition. The results indicate that the absorption coefficient of nanocomposites exhibits an upward trend as the concentration of A1203 NPs increases. This can be attributed to the enhanced absorption of charge carriers in (PMMA/PS/A1203) nanocomposites. The treatment results in an elevation of the absorption coefficients in the augmentation of charge carriers, and bond breakage increases the optical absorption of materials in the visible and near-infrared regions. The given sequence corresponds to the set of integers [26,27,28].

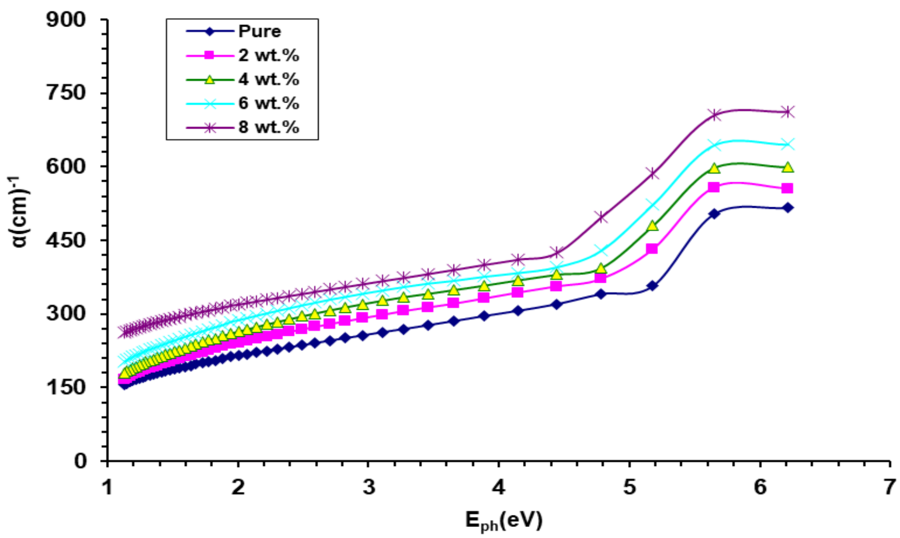

Figure (10): The absorption coefficient of (PMMA/PS/Al_2O_3) NPs.

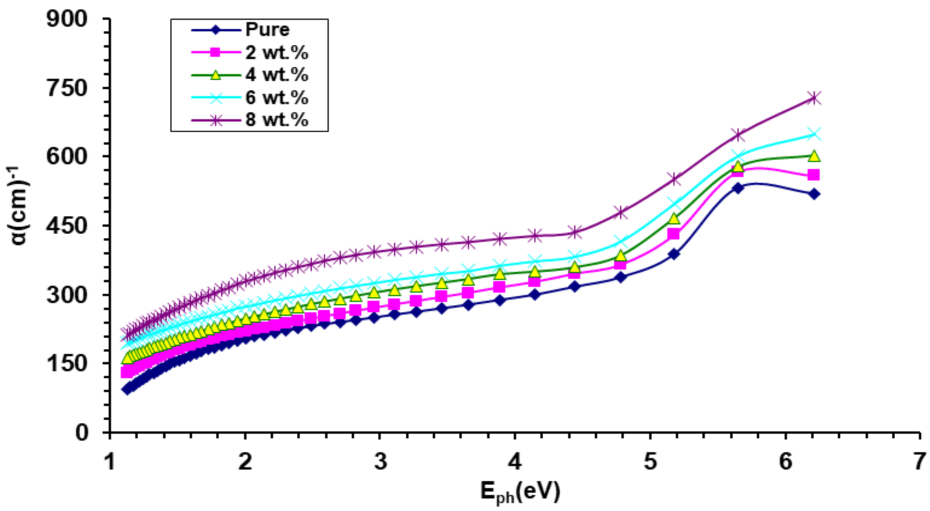

Figure (11): The variation absorption coefficient of (PMMA/PS/Al_2O_3).

The diagrams in Figures 12 and 13 demonstrate the degree of energy release associated with authorized and unauthorized passive transformations of (PMMA/PS/Al2O3) NCS, pre- and post-Argon plasma exposure. The quantity of Al2O3 nanoparticles has been demonstrated to reduce the energy gap. The growth of Poly-methyl-methacrylate/Polystyrene/Aluminum oxide nanocomposite results in a reduction of the thermal gap due. Due to the presence of charge carriers and bond rupture, indirect band separation is diminished for permitted and prohibited treatments. Tables 1 and 2 present the values of the energy gap for both indirect transitions (forbidden and allowed) before and after the emission of Ar particles [26,27].

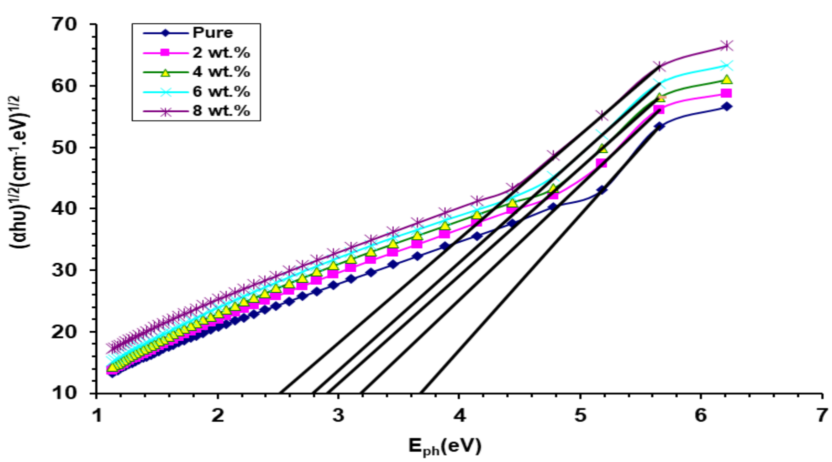

Figure (12): Difference of $(\alpha h\upsilon)^{1/2}$ for of (PMMA/PS/Al_2O_3) with photon energy after exposed Ar plasma.

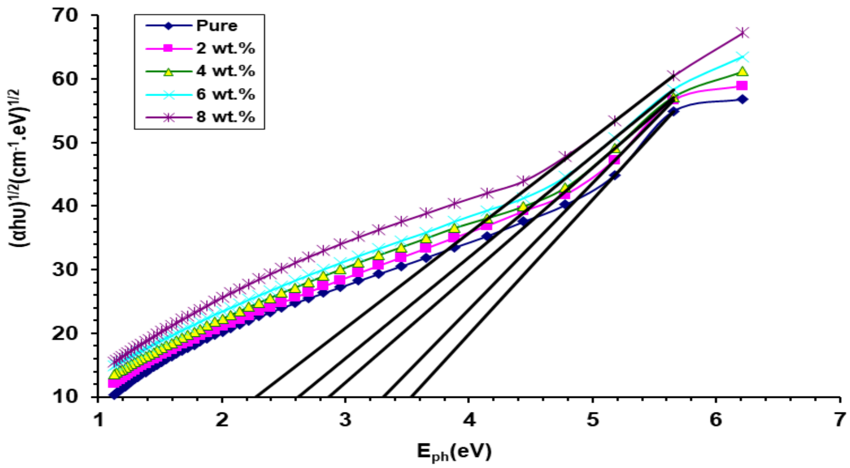

Figure (13): Plot of $(\alpha h\upsilon)^{1/2}$ vs. hυ for ($PMMA/PS/Al_2O_3$) with photon energy.

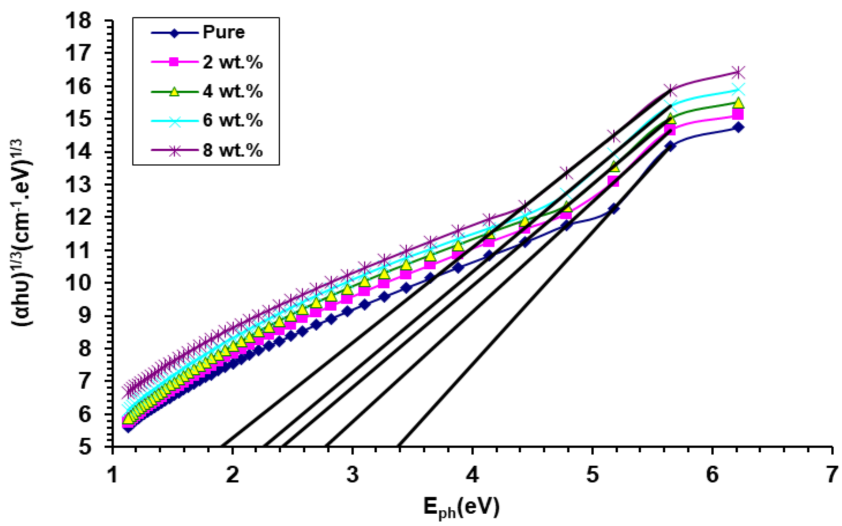

Figure (14): Plot of $(\alpha h\upsilon)^{1/3}$ vs. hυ for ($PMMA/PS/Al_2O_3$).

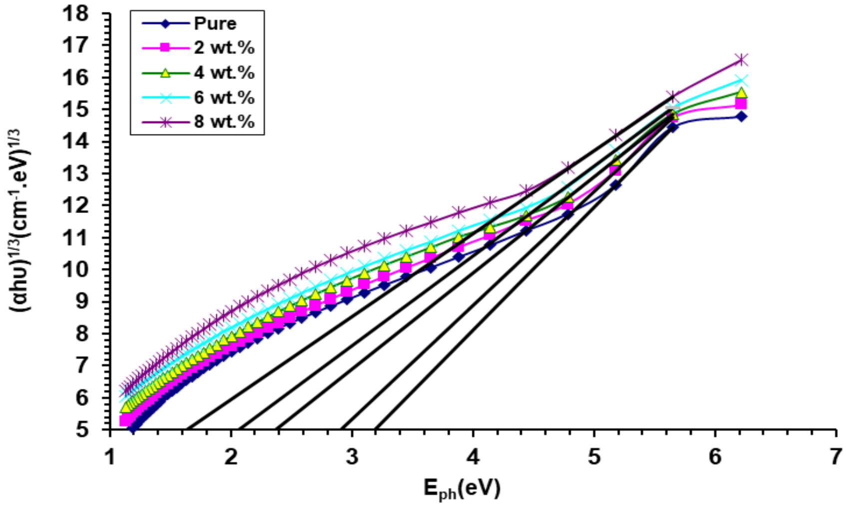

Figure (15): Plot of $(\alpha h\upsilon)^{1/3}$ vs. hυ for (Poly-methyl-methacrylate/Polystyrene/Aluminum oxide) with photon energy after exposed Argon plasma.

Table (1): Values of Eg for Poly-methyl-methacrylate-Polystyrene/Aluminum oxide NCS before exposed Ar plasma.

Al_2O_3	Indirect energy gap (forbidden) eV	Indirect energy gap (allowed) eV
0%	3.38	3.67
2%	2.78	3.19
4%	2.42	2.90
6%	2.28	2.79
8%	1.92	2.52

Table(2): Values of Eg for PMMA-PS/Al_2O_3 NCS after exposed Ar plasma.

Al_2O_3	Indirect energy gap (allowed) eV	Indirect energy gap (allowed) eV
0%	3.20	3.53
2%	2.93	3.31
4%	2.39	2.87
6%	2.09	2.62
8%	1.66	2.29

The extinction coefficient

Figures (16) and (17) depict the extinction coefficient's variation as a function of wavelength, both before and after exposure to Argon plasma, The quantity of (Al2O3)NPS resulted in a reduction of the extinction coefficient. The findings of this study indicate that the observable extinction coefficient experiences an increase after irradiation, which can be attributed to the presence of augmented charge carriers and bond cleavage. These findings are consistent with published researches [26,27,28].

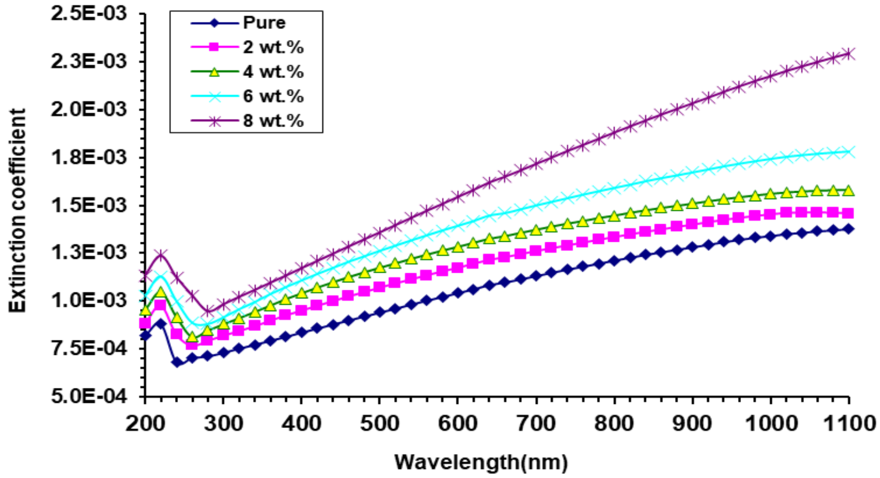

Figure (16): Extinction coefficient for (PMMA/PS/Al_2O_3) NCS.

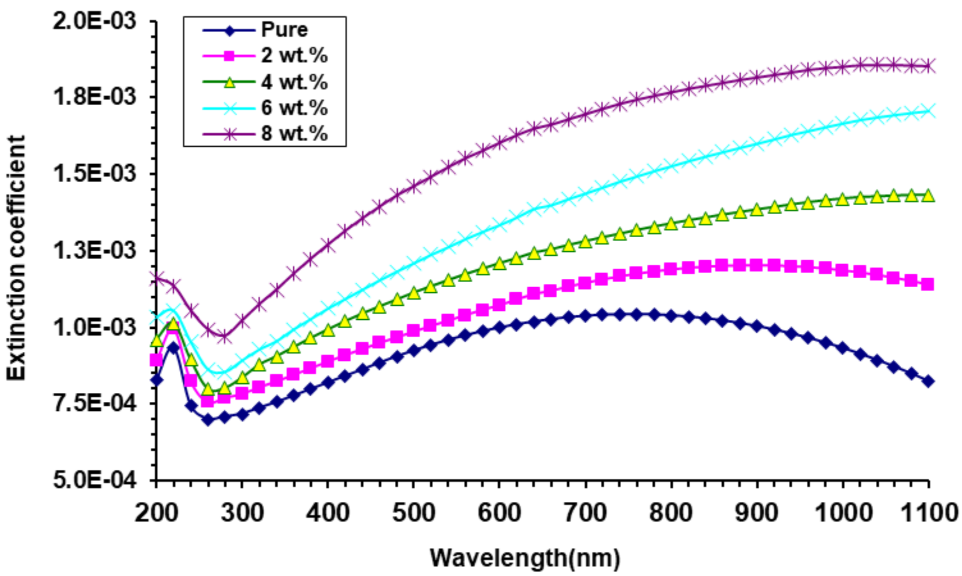

Figure (17): Extinction coefficient for (PMMA/PS/Al_2O_3) NCS after exposed Ar plasma.

The diagrams presented in Figures (18) and (19) depict the variation in the refractive index of (PMMA/PS/ Al_2O_3) NPS concerning wavelength, both prior to and after Ar plasma exposure. The presented data indicate that the concentration of Al2O3 nanoparticles results in an elevation of the refractive index. The density of nanocomposites was observed to increase with the inclusion of Al_2O_3. Based on the presented statistics, it can be inferred that the refractive index experiences a decrease in the visible and near-infrared regions following irradiation. This phenomenon can be attributed to the augmented presence of charge carriers and bond breakage. Academic consensus has been reached among researchers [26,27,29].

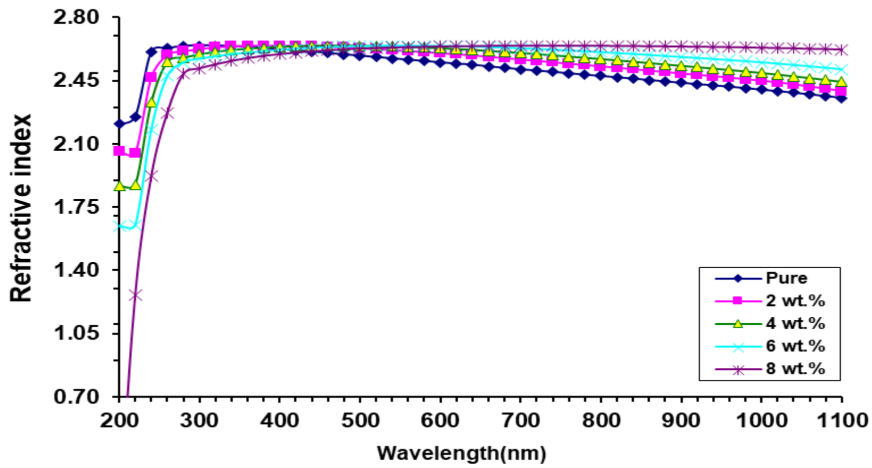

Figure (18): Refractive index of (PMMA/PS/ Al_2O_3) NCS.

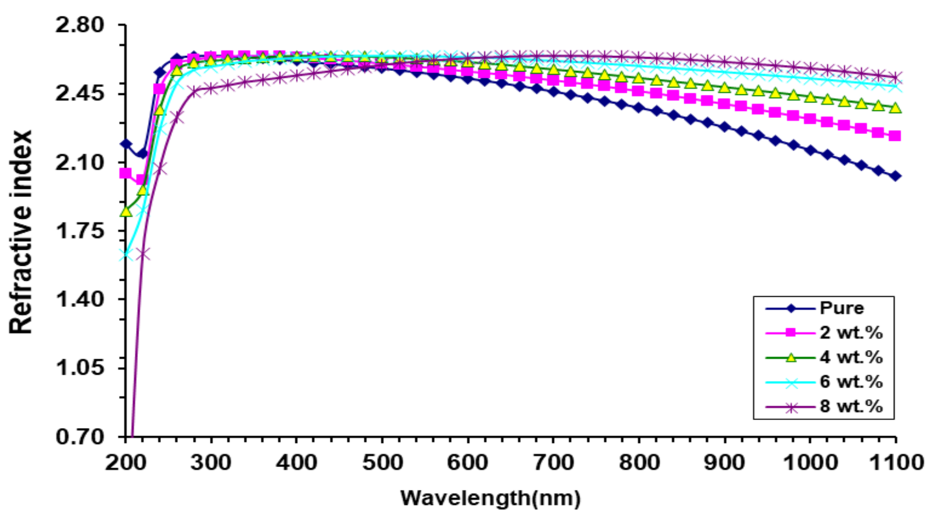

Figure (19): Refractive index of (PMMA/Polystyrene/ Al_2O_3) NC_S after exposed Argon plasma.

The real and imaginary dielectric constant (ε_1 and ε_2)

The real and imaginary dielectric constant of (Poly-methyl-methacrylate/Polystyrene/Aluminum oxide) composites before and after Ar plasma exposure is illustrated in Figure 20. The presented data demonstrate that the incorporation of Al_2O_3 nanoparticles increases both the real and imaginary components of the dielectric constant of the ($PMMA/PS/Al_2O_3$) NCS. The electrical polarisation of the sample was observed to increase due to the presence of nanoparticles [24]. The dielectric constants of nanocomposites exhibit a dependence on the wavelength. In contrast, the latter is contingent upon the refractive index.

The relationship between the imaginary component of the dielectric constant and the extinction coefficient holds substantial importance, especially in the visible and near-infrared wavelengths. Under this particular regime, it can be observed that the refractive index maintains a relatively stable value, whereas the extinction coefficient displays a rising pattern as the wavelength increases [17,18,25].

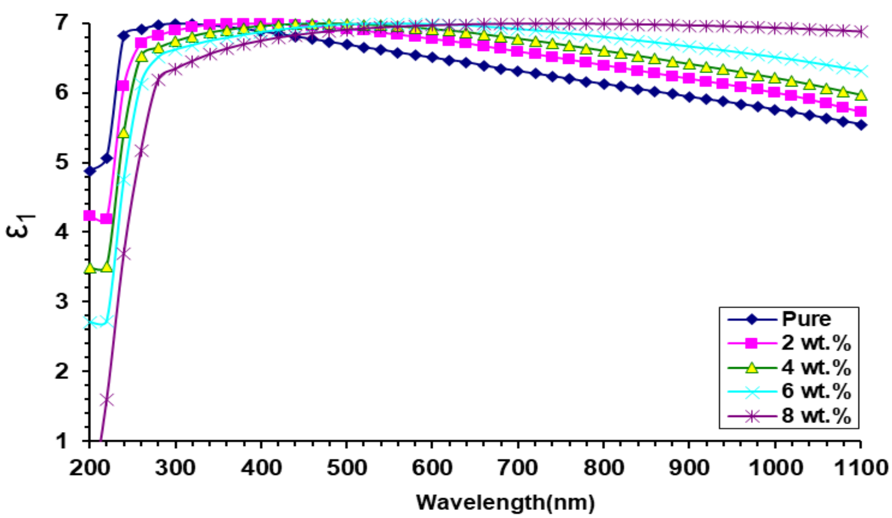

Figure (20): Plot of (ε1) for(Poly-methyl-methacrylate/Polystyrene/Aluminum oxide) NCS.

The optical conductivity and wavelength relationship for ($PMMA/PS/Al_2O_3$) nanocomposites is depicted in figure 16 with consideration to their respective wavelengths, both prior to and following exposure to Argon plasma; as the concentration of Al_2O_3 increases in the (PMMA/PS/Al2O3)NCS. The occurrence of regional platforms within the energy gap results in a rise in the thickness of localized states in the collective arrangement and optical conductance. Materials with higher absorption coefficients tend to exhibit superior optical performance in the context of NPS. The presented data indicate that exposure to UV irradiation elevates charge carriers and bond breakage, leading to an increase in optical conductivity. The outcomes are consistent with existed literature [17,18,26].

3. Conclusion

In the current study, polymer nanocomposites (NCPs) based on a PMMA/PS blend were synthesized by means of a solution casting technique. The surface morphology of the ($PMMA/PS/Al_2O_3$)NCS films is depicted by SEM, which displays a variety of fragments or aggregates scattered at random over the top surface, all of which are consistent and uniform in appearance and optical microscope images indicate of (Al_2O_3) additives distribution was homogeneous and the nanoparticles create a continuous network inside the polymer blend. FTIR analysis revealed that (PMMA/PS/Al2O3)NCS allow for limited vibrational molecular mobility, whereas (Al2O3) nanoparticles destroyed specifc polymer manacles. The increase in nanoparticle concentration of (Al2O3) leads to a rise in both the absorbance and absorption coefficient of ($PMMA/PS/Al_2O_3$) NCs. As the concentration of (Al_2O_3) increases, there is an observed increase in the refractive index, extinction coefficient, dielectric constant (both real and imaginary), and optical conductivity. The inclusion of 8 wt.% of (Al_2O_3) nanofiller resulted in a decrease of the energy gap for indirect transitions, both allowed and forbidden.

Acknowledgments

Thanks and appreciation and gratitude to the University of Babylon and its Department of Physics for their invaluable assistance in the successful completion of this study.

References

[1] Choi BR, Park S-J, Kim S (2015) Preparation of polyethylene oxidecomposite electrolytes containing imidazolium cationsalt-attached titanium oxides and their conducing behavior. J Ind Eng Chem 31:352–359. https://doi.org/10.1016/j.jiec.2015.07.009

[2] Mahdi SM, Habeeb MA (2022) Evaluation of the infuence of SrTiO3 and CoO nanofllers on the structural and electrical polymer blend characteristics for electronic devices. Digest J Nanomater Biostruct 17(3):941–948. https://doi.org/10.15251/DJNB.2022.173.941

[3] Alsaad, A. M., Al-Bataineh, Q. M., Ahmad, A. A., Jum'h, I., Alaqtash, N., & Bani-Salameh,

A. A. (2020). Optical characteristics of transparent PMMA-PS/ZnO NPs polymeric nanocomposite films: UV-Shielding applications. Materials Research Express, 6(12), 126446. https://doi.org/10.1088/2053-1591/ab68a0.

[4] Fatimah T. Al-Hussein, Bahaa H. Rabee,"study of some electrical characteristics (PS/TiO2/AL2O3) nanocomposite film injected with air nanobubbles for antibacterial application" HIV nursing, Vol.2, No.22, pp.1621.1624, 2022. https://doi.org/10.31838/hiv22.02.310.

[5] Maeda, S., Fujita, M., Idota, N., Matsukawa, K., & Sugahara, Y. (2016). Preparation of transparent bulk TiO2/PMMA hybrids with improved refractive indices via an in situ polymerization process using TiO2 nanoparticles bearing PMMA chains grown by surface-initiated atom transfer radical polymerization. ACS applied materials & interfaces, 8(50), 34762-34769. https://doi.org/10.1021/acsami.6b10427.

[6] Angham Hazim, Hayder M. Abduljalil, Ahmed Hashim, Structural, Spectroscopic, Electronic and Optical Properties of Novel Platinum Doped (PMMA/ZrO2) and (PMMA/Al2O3) Nanocomposites for Electronics Devices, Transactions on Electrical and Electronic Materials [2020), https://doi.org/10.1007/s42341-020-00210-2.

[8] Alsaad, A., Al Dairy, A. R., Ahmad, A., Qattan, I. A., Al Fawares, S., & Al-Bataineh, Q. (2021). Synthesis and Characterization of Polymeric (PMMA-PVA) Hybrid Thin Films Doped with TiO2 Nanoparticles Using Dip-Coating Technique. Crystals, 11(2), 99. https://doi.org/10.3390/cryst11020099.

[9] Meteab, M.H., Hashim, A. & Rabee, B.H. Controlling the Structural and Dielectric Characteristics of PS-PC/Co_2O_3-SiC Hybrid Nanocomposites for Nanoelectronics Applications. Silicon 15, 251–261 (2023). https://doi.org/10.1007/s12633-022-02020-y.

[10] Meteab, M.H., Hashim, A. & Rabee, B.H. Synthesis and Characteristics of SiC/MnO2/PS/PC QuaternaryNanostructures for Advanced Nanodielectrics Fields. Silicon 15, 1609–1620 (2023). https://doi.org/10.1007/s12633-022-02114-7.

[11] Shamala, K. S., Murthy, L. C. S., & Rao, K. N. (2004). Studies on optical and dielectric characteristics of Al2O3 thin films prepared by electron beam evaporation and spray pyrolysis method. Materials Science and Engineering: B, 106(3), 269-274. https://doi.org/10.1016/j.mseb.2003.09.036.

[12] Papancea A., Patachia S. (2015). Characterization of Dyes Loaded Polyvinyl Alcohol (PVA) Based Hydrogels through CIELAB Method, Environmental Engineering and Management Journal, 14(2): 361-371. https://doi.org/10.30638/eemj.2015.037.

[13] AL-Kadhemy, M. F. H., Ibrahim, S. A., & Salman, J. A. S. (2020, December). Studying the physical characteristics polyvinyl alcohol polymer mixture with silica nanoparticles and its application as pathogenic bacteria inhibitor.

In AIP Conference Proceedings (Vol. 2290, No. 1, p. 050013). AIP Publishing LLC. https://doi.org/10.1063/5.0028817

[14] M. Jothibas, C. Manoharan, S. Johnson Jeyakumar, P. Praveen, Study on structural and optical behaviors of In2O3 nanocrystals as potential candidate for optoelectronic devices. J Mater Sci: Mater Electron, Vol.26, pp.9600–9606, (2015), https://doi.org/10.1007/s10854-015-3623-x.

[15] T. Abdel-Baset, M. Elzayat, and S.Mahrous, Characterization and Optical and Dielectric Characteristics of Polyvinyl Chloride/Silica Nanocomposites Films, International Journal of Polymer Science, Vol. 2016, Article ID 1707018, 13 pages, http://dx.doi.org/10.1155/2016/1707018

[16] Shalini Agarwal, Y. K. Saraswat and Vibhav K. Saraswat, Study of Optical Constants of ZnO Dispersed PC/PMMA Blend Nanocomposites, Open Physics Journal, Vol.3, pp.63-72, (2016), http://dx.doi.org/10.2174/1874843001603010063.

[17] N. Mahfoudh, K. Karoui and A. Ben Rhaiem, Optical studies and dielectric response of [DMA]2MCl4 (M ¼ Zn and Co) and [DMA]2ZnBr4, RSC Adv., Vol.11, (2021), http://dx.doi.org/10.1039/d1ra03652a.

[18] A. Alsaad, A. R. Al Dairy, A. Ahmad, I. A. Qattan, S. Al Fawares and Q. Al-Bataineh, Synthesis and Characterization of Polymeric (PMMA-PVA) Hybrid Thin Films Doped with TiO2 Nanoparticles Using Dip-Coating Technique, Crystals, Vol.11, (2021), https://doi.org/10.3390/cryst11020099.

[19] Meteab, M.H., Hashim, A. & Rabee, B.H. Synthesis and tailoring the morphological, optical, electronic and photodegradation characteristics of PS–PC/MnO2–SiC quaternary nanostructures. Opt Quant Electron 55, 187 (2023). https://doi.org/10.1007/s11082-022-04447-4.

[20] A. Paydayesh, A. A. Azar and A. J. Arani, "Investigation the effect of Graphene on The Morphology, Mechanical and Thermal properties of PLA/PMMA Blends, " Ciência Natura, Vol. 37, pp. 15-22, (2015)

[21] T. S. Praveenkumar, J. S. Ashwajeet and R. Ramanna, “Dielectric and AC Conductivity Studies in PPy-Ag Nanocomposites” Journal of Polymers, Vol.2015, 2015).

[22] M. Rezvanpour, M. Hasanzadeh, D. Azizi, A. Rezvanpour and M. Alizadeh, “Synthesis and characterization of micro-nanoencapsulated n-eicosane with PMMA shell as novel phase change materials for thermal energy storage” Mater. Chem. Phys., Vol. 215, pp. 299–304, (2018).

[23] A. A. Mohaimeed, B. H. Rabee, "Influence of Berry dye on some properties of nanocomposite (PVA/TiO2) films". Opt Quant Electron, Vol. 55, p.254, (2023)

[24] H. Shivashankar, K. A. Mathias, P. R. Sondar, M. H. Shrishail, and S. M. Kulkarni, "Study on low-frequency dielectric behavior of the carbon black/polymer nanocomposites", J Mater Sci: Mater Electron, Vol.32, (2021).

[25] C. Srikanth, B. C. Sridhar, M. V. N. Prasad and R. D. Mathad, "Characterization and DC conductivity of novel ZnO doped polyvinyl alcohol (PVA) nanocomposite films" Journal of Advanced Physics, Vol. 5, No.2, pp.105-109, (2016).

[26] N. Mahfoudh, K. Karoui and A. Ben Rhaiem, Optical studies and dielectric response of [DMA]2MCl4 (M ¼ Zn and Co) and [DMA]2ZnBr4, RSC Adv., Vol.11, (2021), http://dx.doi.org/10.1039/d1ra0365.